Preparation and Characterization of Carrot Nanocellulose and Ethylene/Vinyl Acetate Copolymer-Based Green Composites

Yu-Cian Ke[1], Ying-Chieh Chao[2], Chun-Wei Chang[1], Yeng-Fong Shih[1,*]

[1]Department of Applied Chemistry, Chaoyang University of Technology, Taichung, Taiwan, ROC

[2]Material and Chemical Research Laboratories, Industrial Technology Research Institute, Hsinchu, Taiwan, ROC

Received 04 June 2023; received in revised form 29 August 2023; accepted 30 August 2023

DOI: https://doi.org/10.46604/ijeti.2023.12375

Abstract

This study aims to investigate the effect of nanocellulose on the properties and physical foaming of ethylene/vinyl acetate (EVA) copolymer. The nanocellulose is prepared from waste carrot residue using the 2,2,6,6-tetramethylpiperidine-1-oxyl (TEMPO) oxidation method (CT) and is further modified through suspension polymerization of methyl methacrylate (MMA) monomer (CM). The obtained nanocellulose samples (CT or CM) are added to EVA to create a series of nanocomposites. Moreover, the EVA and CM/EVA composite were further foamed using supercritical carbon dioxide physical foaming. TEM results show that the average diameters of CT and CM are 24.35 ± 3.15 nm and 30.45 ± 1.86 nm, respectively. The analysis of mechanical properties demonstrated that the tensile strength of pure EVA increased from 10.02 MPa to 13.01 MPa with the addition of only 0.2 wt% of CM. Furthermore, the addition of CM to EVA enhanced the melt strength of the polymer, leading to improvements in the physical foaming properties of the material. The results demonstrate that the pore size of the CM/EVA foam material is smaller than that of pure EVA foam. Additionally, the cell density of the CM/EVA foam material can reach 3.23×10^{11} cells/cm^3.

Keywords: carrot, nanocellulose, ethylene/vinyl acetate copolymer, physical foaming

1. Introduction

Due to the issue of global warming and the goal of achieving net-zero carbon emissions, using plant fibers with carbon-neutral benefits as a substitute for synthetic fibers is one method for developing low-carbon materials. Various applications of biomass toward carbon neutrality have been investigated [1]. Plant fibers primarily consist of cellulose, hemicellulose, lignin, and pectin. In general, there is 30-50 % of carrot waste produced in the carrot juice production process. The cellulose content in carrot waste is as high as 81 % [2]. If carrot waste is used as raw material to produce nanocellulose, not only can achieve recycling economics, but its additional value can also be increased.

In recent years, many studies have utilized carrot residue to prepare nanocellulose and incorporated carrot nanofibers into composites to enhance the material's mechanical strength [3]. Nanocellulose is a renewable and environmentally friendly nanomaterial that possesses a favorable combination of properties required in wearable technologies, including deformability, printability, high mechanical resistance, and lightweight nature [4]. There are many methods to prepare nanocellulose, such as acid hydrolysis, mechanical methods, and 2,2,6,6-tetramethylpiperidine-1-oxyl (TEMPO)-mediated oxidation. Among them, nanocellulose prepared using the TEMPO-mediated oxidation method possesses the advantage of having a high aspect ratio, which makes its reinforcement effect more prominent [5]. Saito et al. [6] employed the TEMPO radical oxidation method to treat plant fibers, facilitating oxidation on the cellulose surface and catalyzing the hydroxyl groups into carboxyl groups.

* Corresponding author. E-mail address: syf@cyut.edu.tw

English language proofreader: Chih-Wen Teng

Furthermore, after oxidation, the fibers acquired a negative charge and were reduced to the nanometer scale [6-7]. Nanocellulose offers advantages such as a high aspect ratio, strength, rigidity, low density, lightweight, large surface area, and biocompatibility. Additionally, the addition of nanocellulose can maintain material transparency without affecting its appearance. Currently, nanocellulose finds a wide range of applications in environmental engineering, flexible electronics, biosensors, and other fields [8-9].

Ethylene/vinyl acetate (EVA) copolymer is the fourth largest vinyl copolymer in terms of usage, following high-density polyethylene (HDPE), low-density polyethylene (LDPE), and linear low-density polyethylene (LLDPE). EVA is an elastomeric polymer that imparts a "rubber-like" softness and flexibility to materials. It has found extensive applications in footwear components, flexible hoses, automobile bumpers, toys, flexible packaging, and films [10]. However, the mechanical strength of EVA is not sufficient and can be enhanced through polymer blending or the addition of fillers [11-12].

There are three commonly used methods for polymer foaming: chemical, physical, and mechanical. Cross-linked EVA foam materials are extensively utilized in sporting goods, thermal insulation materials, cushioning fillers, and various everyday necessities [13-14]. This is due to their lightweight nature, good elasticity, and affordability.

However, once EVA foam material is cross-linked, it becomes non-recyclable and difficult to process, leading to environmental waste accumulation. Physical foaming using supercritical fluids [15-16], with supercritical carbon dioxide fluid being the most commonly used solvent, offers a potential solution. The advantages of physical foaming with supercritical fluids include (1) supercritical temperatures close to room temperature, (2) non-toxicity, (3) gas-like viscosity, (4) liquid-like density, (5) high mass transfer efficiency, and (6) tunable solubility with temperature and pressure. Furthermore, the resulting foamed material can be recycled using chemical or physical methods, making it more environmentally friendly than chemical approaches.

In their research, Ren et al. [17] employed the incorporation of nanocellulose into a polylactic acid (PLA) substrate to address the drawbacks of its low melt strength and slow crystallization rate. The results demonstrated that the rheological properties of the composite with unmodified nanocellulose exhibited minimal improvement at 180 °C, whereas the addition of modified nanocellulose exhibited a noticeable enhancement. Scanning electron microscope (SEM) analysis revealed that the cell size of the PLA foam material was significantly reduced when nanocellulose was added during the foaming process at temperatures ranging from 100 °C to 140 °C. This suggests that incorporating nanocellulose could significantly improve the viscoelasticity and melt strength of PLA.

The study focused on examining the effects of nanocellulose on the properties and supercritical carbon dioxide foaming behavior of the composites. In this study, industrial waste carrot residue was utilized and subjected to the TEMPO radical oxidation method to produce nanocellulose. Furthermore, the surface of the nanocellulose was modified through suspension polymerization of methyl methacrylate (MMA) monomer, aiming to enhance the compatibility and dispersibility of nanocellulose when combined with EVA. Consequently, the unmodified and modified carrot nanocelluloses were incorporated into EVA to create environmentally friendly nanocomposites. Furthermore, the EVA and nanocellulose/EVA composite were foamed using supercritical carbon dioxide physical foaming, and the effects of adding nanocellulose on the density, pore size, and cell density of EVA foamed materials were investigated.

2. Materials and Methods

This section provides the materials and methods for preparing alkaline-treated carrot cellulose, bleached carrot cellulose, TEMPO-oxidized carrot nanocellulose, MMA-modified carrot nanocellulose, nanocellulose/EVA composites, and EVA foam materials. Additionally, the analysis procedures for the materials' morphology, hydrophilic properties, and tensile strength were described.

2.1. Materials

The EVA pellets (7470M) were provided by Formosa Plastics Co., Taipei, Taiwan. Carrot residue was obtained from Vigor Dong Shih, Taiwan. Sodium hydroxide (NaOH), hydrochloric acid (HCl), and sodium hypochlorite (NaClO) were supplied by Echo Chemical Co., Ltd., Miaoli, Taiwan. TEMPO and polyvinyl alcohol (PVA) were purchased from Sigma-Aldrich Co., Darmstadt, Germany. MMA, 2,2'-azobis (2-methylpropionitrile) (AIBN), and sodium chlorite ($NaClO_2$) were obtained from Aldrich Chemical Co. and used as received. All materials were used without further purification or modification. The physical blowing agent, CO_2 (99 % purity), was provided by Linde LienHwa Corporation.

2.2. Preparation of alkaline-treated carrot cellulose

The obtained carrot residue (C) underwent several surface chemical modifications using the following procedures: First, the carrot residue was washed and dried in a vacuum oven at 80 °C. Subsequently, it was treated with a 5 % NaOH solution for 45 minutes to eliminate lignin, hemicellulose, and impurities. Next, the residue was neutralized with a 1 % acetic acid solution and rinsed with running tap water, followed by distilled water until the pH value reached 7.0. This resulted in the production of alkaline-treated carrot cellulose (CA).

2.3. Preparation of bleached carrot cellulose and carrot nanocellulose

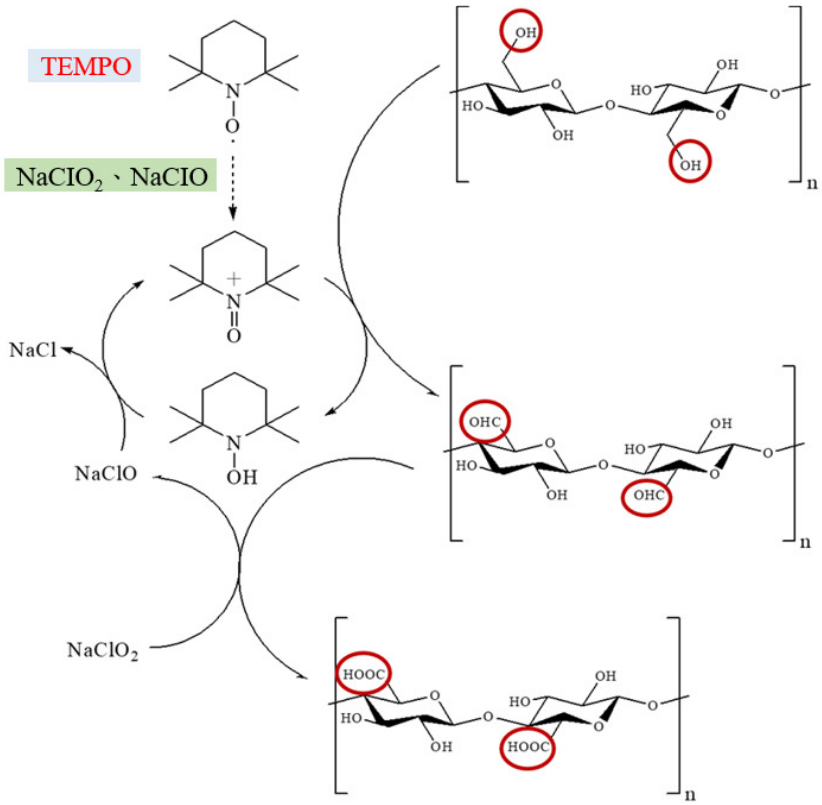

Fig. 1 TEMPO radical oxidation method

The carrot nanocellulose was synthesized via the TEMPO radical oxidation method, a procedure outlined in the work of Saito and Isogai [6], with further details provided in Isogai et al.'s [7] study and exemplified in Fig. 1. Initially, the CA obtained previously was subjected to bleaching. This involved placing CA in an acetate buffer solution with 0.4 % $NaClO_2$ at pH 4.8 and heating it at 85 °C with agitation at 400 rpm for 4 hours. Then, most lignin and hemicellulose will be removed after alkaline-treatment and bleaching process [18]. The resulting material, known as bleached carrot cellulose (CO), was then further modified through TEMPO radical oxidation. Specifically, 3 g of CO was suspended in a sodium phosphate buffer (90 mL, pH 6.8). To this suspension, 1.13 g of $NaClO_2$ (80 %) and 0.016 g of TEMPO were added. Additionally, 0.5 mL of a 2M

NaClO solution was diluted to 0.1 M using the aforementioned buffer and added to the mixture. The reaction proceeded at 60 °C with agitation at 400 rpm for 4 hours. Following the reaction, the resulting TEMPO-oxidized carrot nanocellulose (CT) was thoroughly washed with water (100 mL) through filtration and subsequently freeze-dried before further treatment.

2.4. *Surface modification of carrot nanocellulose*

The MMA monomer, initiator (AIBN), and dispersant (PVA) were combined in a ratio of 1:0.05:0.03 and thoroughly mixed. Subsequently, 1.5 g of CT was added to the mixture, and the stirring continued at 75 °C with an agitation speed of 400 rpm for 6 hours. Following the reaction, the resulting mixture was washed and filtered using water and acetone. The obtained MMA-modified carrot nanocellulose (CM) was then freeze-dried for further use in composite fabrication [19]. The preparation procedure for CM is illustrated in Fig. 2, while the diagram representing the steps is depicted in Fig. 3 [20].

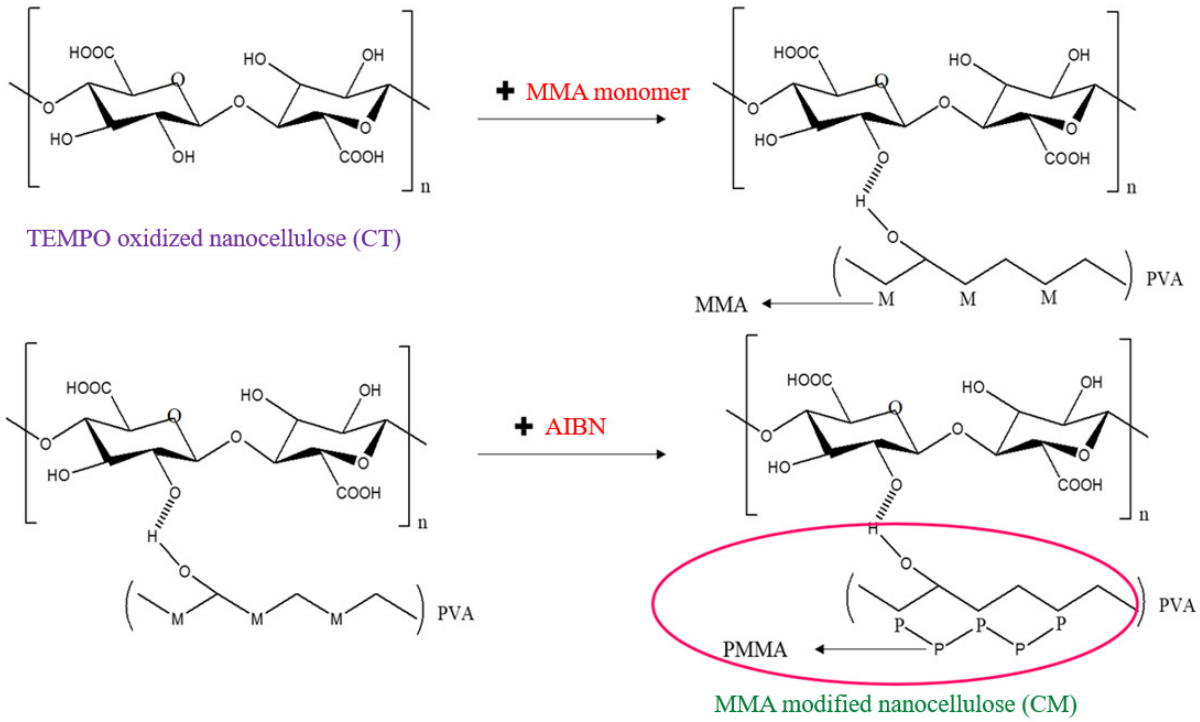

Fig. 2 Preparation procedure of MMA modified carrot nanocellulose

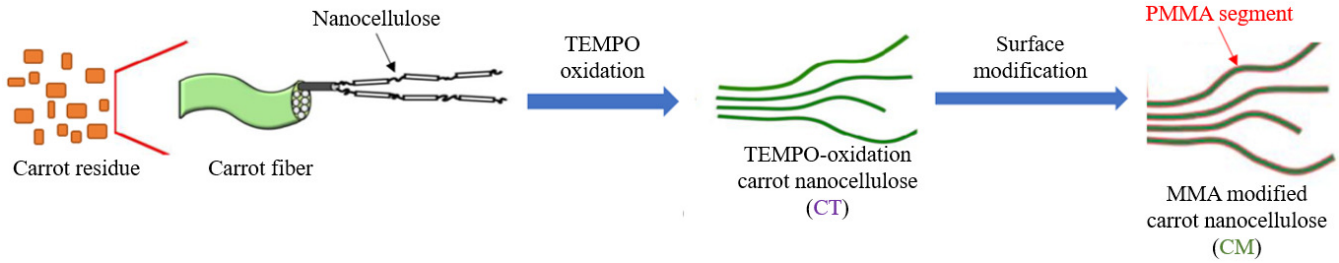

Fig. 3 Preparation diagram of TEMPO-oxidized carrot nanocellulose and MMA modified carrot nanocellulose

2.5. *Preparation of nanocellulose/EVA green composites*

The EVA and nanocelluloses (CT or CM) were dried in a vacuum oven at 100 °C for 4 hours until the moisture content was below 1.0 wt%. Subsequently, the EVA was melt-blended with the nanocelluloses in a counter-rotating internal mixer (Brabender PL2000, Duisburg, Germany) at 85 °C for 5 minutes, with a rotation speed of 50 rpm. Different loadings of CT or CM, 0.1, 0.2, and 0.3 wt%, were added to the EVA and labeled as CT0.1, CT0.2, CT0.3, CM0.1, CM0.2, and CM0.3, respectively. The resulting mixtures were then subjected to compression molding at 85 °C for 5 minutes under a pressure of 25 kg_f/cm^2, followed by 3 minutes under 45 kg_f/cm^2, and finally 1 minute under 65 kg_f/cm^2.

2.6. Preparation of EVA and CM0.1 foam materials

The foaming process was carried out using a supercritical fluid foaming machine designed by the Industrial Technology Research Institute (ITRI) in Hsinchu, Taiwan [21]. To initiate the foaming process, either EVA or CM0.1 was first placed in the mold. Subsequently, the foaming mold was heated to specific temperatures of 30, 40, or 50 °C. Once the mold reached the desired temperature, it was closed, and CO_2 was pumped into the mold cavity, displacing the air present inside.

This pumping and venting process was repeated three times. Afterward, CO_2 was pumped into the mold cavity and the pressure was maintained at 2000, 2500, or 3000 psi. The samples were then saturated with the supercritical fluid at the specified temperature and pressure for a duration of 30, 60, or 90 minutes. Subsequently, the pressure relief valve was quickly opened to release the pressure, resulting in the formation of foam materials (see Fig. 4) [22].

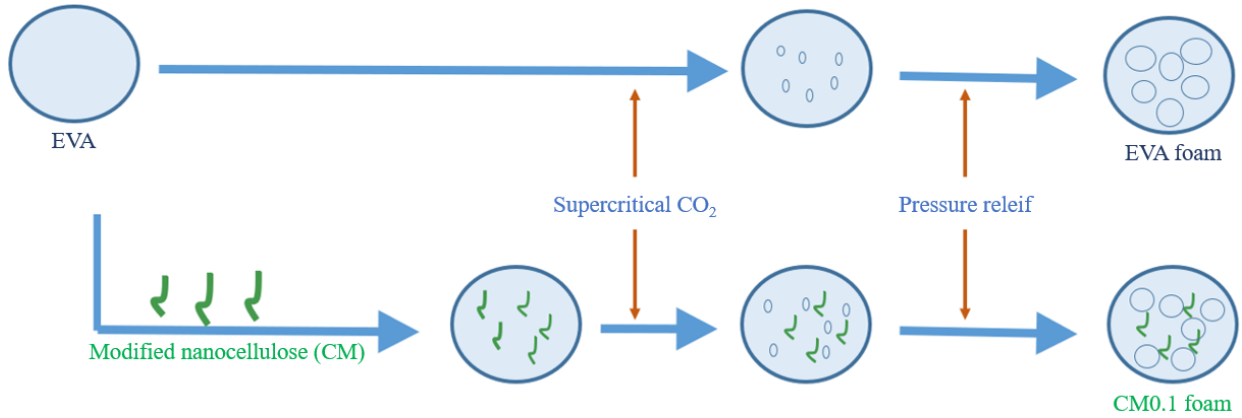

Fig. 4 Diagram of the physical foaming system used in the study

2.7. Characterization

Transmission electron microscopy (TEM) observations of the nanocellulose were conducted using a JEOL JEM-2010 microscope operating at an acceleration voltage of 200 kV. X-ray diffractometry (XRD) measurements were performed using a Rigaku D/MAX-2200PC X-ray diffractometer with Cu Kα radiation (wavelength: 0.154 nm). The instrument operated at 40 kV and 100 mA, and data were collected within the scattering angle (2θ) range of 5-50°. The hydrophilic property of the carrot nanocellulose was evaluated using a contact angle analyzer (FTA125, First Ten Ångstroms, Inc., Virginia, USA). Deionized water was used as the probing liquid, and wettability was characterized by measuring the contact angle between the solid surface and calibrated drops deposited on the substrate surface.

The transmittance of a nanocomposite (with a sample thickness of 1 mm) was measured using ultraviolet and visible spectroscopy (SPECORD 200, Analytic Jena AG, Jena, Germany). Tensile tests were performed according to ASTM D368 specifications. Dumbbell-shaped test specimens were prepared as per the requirements and stretched using a universal testing machine at a rate of 50 mm/min. The density of the foam material was determined using an electronic densitometer (AU-300PF, Quarrz) following ASTM D3574 standards. Scanning electron microscopy (XL-30 ESEM FEG, Holland FEL Company) was employed to characterize the pore size of the foam material. Based on the obtained measurement data, the cell density was calculated using the formula:

$$N = \left(\frac{n}{A}\right)^{\frac{3}{2}} \frac{\rho}{\rho_f} \tag{1}$$

where n is the number of cells in the SEM image, A is the area of the SEM image, ρ is the density of the EVA and CM0.1, and ρ_f is the density of the foamed EVA and CM0.1.

3. Results and Discussion

In this section, various celluloses were compared using TEM, XRD, and contact angle analysis. Additionally, light transmittance analysis and the tensile strength of nanocellulose/EVA composites were discussed. Subsequently, the supercritical CO_2 foaming process of nanocellulose/EVA composites at different temperatures, pressures, and times was investigated. The effects of adding nanocellulose on the morphology, density, pore size, and cell density of EVA foam were also discussed.

3.1. TEM analysis

It can be observed from the TEM analysis diagrams (Fig. 5) that the average diameters of the unmodified (Fig. 5(a)) and modified (Fig. 5(b)) carrot nanocellulose were 24.35±3.15 nm and 30.45±1.86 nm, respectively. This indicates that the successful grafting of MMA on the surface of the nanocellulose increased the diameter of the nanocellulose. Furthermore, both CT and CM exhibited diameters below 100 nm, indicating their classification on the nanometer scale.

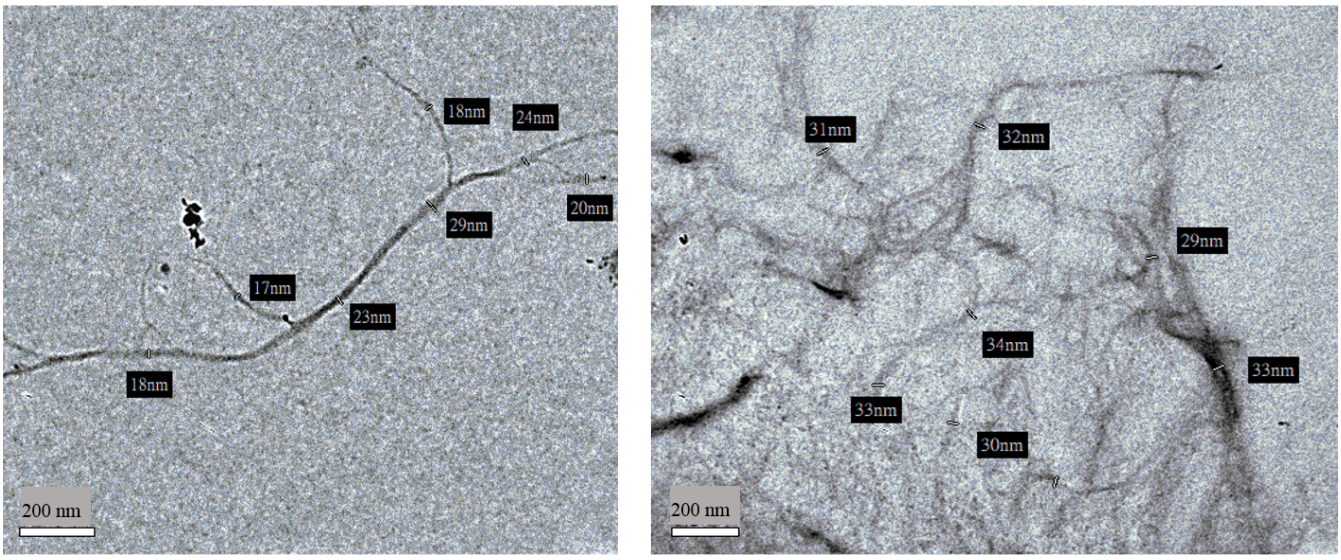

(a) CT (b) CM

Fig. 5 TEM analysis diagrams

3.2. XRD analysis

Fig. 6 displays the XRD diagram of carrot cellulose at each stage. The peak observed at approximately 19.04° of 2θ corresponds to the amorphous phase, while the peaks at 15.36°, 22.20°, and 34.00° correspond to the crystal surfaces (100), (200), and (001), respectively, indicating the characteristic structure of cellulose I [23-24]. The intensity of the peaks at around 15.36° and 22.20° gradually increases with each treatment, while the intensity of the peak at approximately 19.04° decreases with alkali treatment and TEMPO oxidation. The crystallinity indices of C, CA, CO, CT, and CM were determined as 17.78 %, 30.57 %, 42.58 %, 50.83 %, and 15.30 %, respectively. These results reveal that the series of treatments effectively remove lignin and hemicellulose from the amorphous region and gradually improve crystallinity. However, the MMA modification leads to a decrease in the crystallinity of the nanocellulose due to the coverage of the amorphous PMMA layer [25].

3.3. Contact angle analysis

The contact angle refers to the angle between the liquid/gas interfaces on a solid surface and can be used to analyze the hydrophilicity/hydrophobicity of carrot nanocellulose. According to the contact angle analysis (Fig. 7), the values for CT and CM are 16.90° and 63.73°, respectively. Comparing the contact angle of CM to CT, the increased contact angle confirms the success of the modification and indicates that the surface of carrot nanocellulose becomes more hydrophobic.

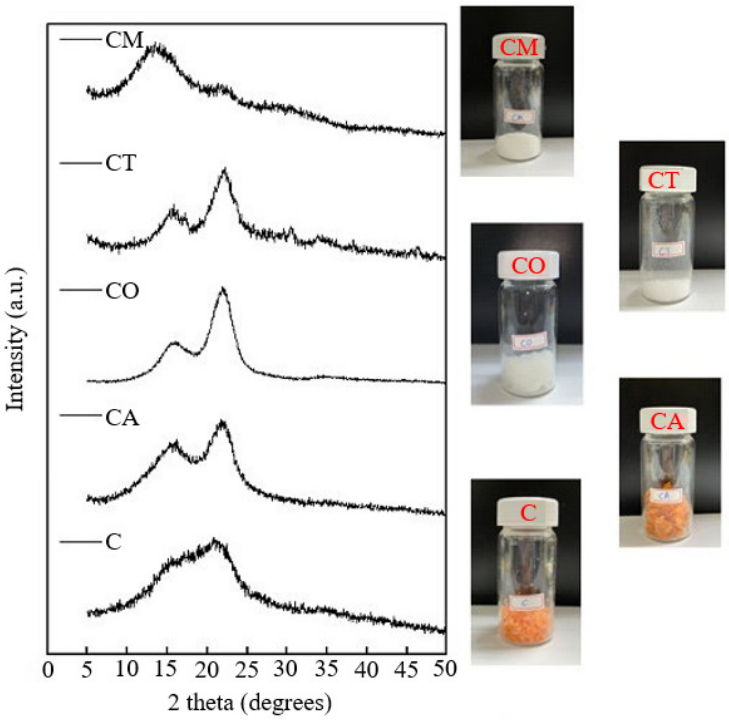

Fig. 6 XRD diagrams of carrot cellulose at each stage

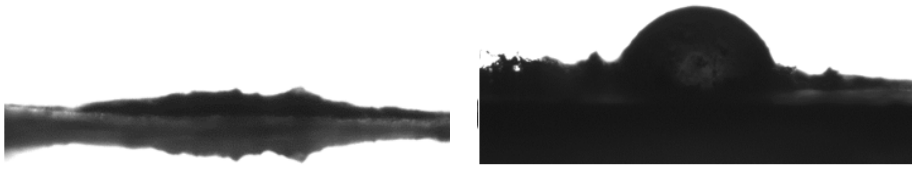

(a) CT (b) CM

Fig. 7 Contact angle of carrot nanocellulose

3.4. Light transmittance analysis

The advantage of nanocomposites is that they can reinforce materials while still maintaining their transparency. Fig. 8 illustrates the light transmittance of pure EVA and nanocomposite films within the wavelength range of 380 nm to 750 nm. The composite film containing 0.2 % or 0.3 % modified nanocellulose (CM0.2 or CM0.3) exhibits higher light transmittance compared to pure EVA. Conversely, the transmittance of the composite film with 0.2 % or 0.3 % unmodified nanocellulose (CT0.2 or CT0.3) is slightly lower than that of pure EVA. This observation suggests that the modified nanocellulose is well dispersed within the pure EVA matrix, resulting in enhanced transparency. Additionally, the light transmittance of CM0.2 was higher than that of CM0.3. It is speculated that the less even dispersion of CM in CM0.3 than that in CM0.2.

3.5. Tensile strength

The advantage of nanocellulose is that it can reinforce the mechanical properties of the material with a small amount added. Fig. 9 displays the tensile strength of pure EVA, which was 10.02±0.47 MPa. Furthermore, the addition of CT or CM to the nanocomposites resulted in increased tensile strengths. However, the tensile strengths of CT0.3 and CM0.3 were lower than those of CT0.2 and CM0.2, respectively. It is speculated that a large amount of nanocellulose leads to uneven dispersion within the matrix, thereby reducing the tensile strength. The tensile strengths of the MMA-modified nanocellulose-reinforced composites (11.51, 13.01, and 12.13 MPa) were significantly higher than those of the unmodified nanocellulose-reinforced ones (10.22, 11.30, and 10.51 MPa). This improvement can be attributed to the improved compatibility between the nanocellulose and EVA after surface modification. The enhanced compatibility reduces the uneven dispersion of the nanocellulose in the substrate, leading to the increased mechanical strength of the composites.

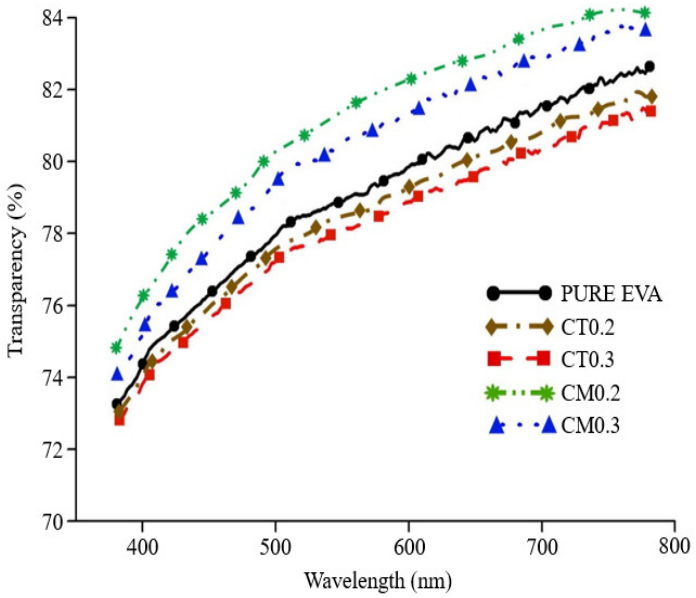

Fig. 8 Light transmittance of PURE EVA and nanocomposite films

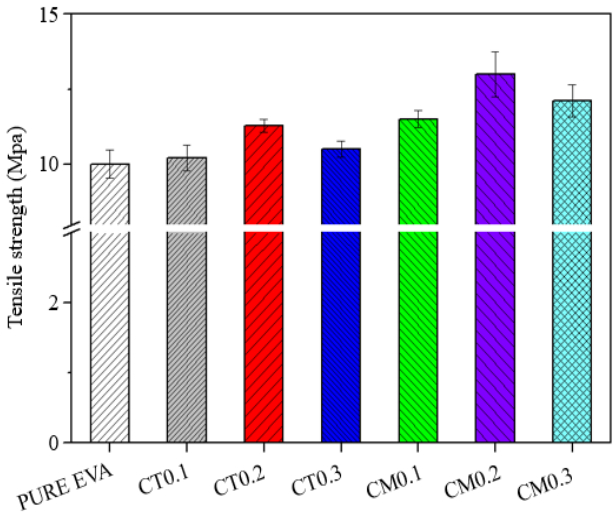

Fig. 9 Tensile strength of EVA and its nanocomposites

3.6. *Supercritical CO_2 foaming*

The foamed materials produced by physical foaming using supercritical carbon dioxide fluid can be recycled, making them more environmentally friendly than chemical foaming ones. Due to the variables in physical foaming, such as temperature, pressure, and time, and considering cost and time constraints, this study initially conducted research using CM0.1 for comparison with pure EVA. Table 1 presents the results of supercritical CO_2 foaming conducted on pure EVA and CM0.1 at temperatures of 30, 40, and 50 °C, and pressures of 2000, 2500, and 3000 psi for 30, 60, and 90 minutes, respectively.

Table 1 Supercritical CO_2 foaming results of pure EVA and CM0.1

Sample	Pure EVA			CM0.1		
Properties / Condition	Density (g/cm^3)	Pore size (μm)	Cell density ($cells/cm^3$)	Density (g/cm^3)	Pore size (μm)	Cell density ($cells/cm^3$)
A. 30 °C; 2000 psi; 30 min	0.669	2.86 ± 1.66	3.49×10^{10}	0.529	1.78 ± 0.32	2.57×10^{11}
B. 30 °C; 3000 psi; 30 min	0.591	2.41 ± 1.26	8.37×10^{10}	0.491	1.93 ± 0.40	1.84×10^{11}
C. 30 °C; 2000 psi; 90 min	0.603	1.90 ± 0.80	1.61×10^{10}	0.511	1.74 ± 0.49	2.10×10^{11}
D. 30 °C; 3000 psi; 90 min	0.540	1.91 ± 0.64	2.10×10^{11}	0.531	2.04 ± 0.37	2.21×10^{11}
E. 40 °C; 2500 psi; 60 min	0.364	2.94 ± 1.31	1.61×10^{10}	0.325	2.10 ± 0.68	2.86×10^{11}
F. 50 °C; 2000 psi; 30 min	0.234	4.30 ± 1.81	8.31×10^{10}	0.339	2.38 ± 0.57	2.31×10^{11}
G. 50 °C; 3000 psi; 30 min	0.271	2.41 ± 1.57	8.37×10^{10}	0.228	3.57 ± 1.15	9.18×10^{10}
H. 50 °C; 2000 psi; 90 min	0.266	4.77 ± 1.97	2.82×10^{10}	0.240	2.35 ± 0.48	3.23×10^{11}
I. 50 °C; 3000 psi; 90 min	0.223	5.17 ± 2.56	4.55×10^{10}	0.193	2.79 ± 0.75	2.16×10^{11}

Regardless of whether it is EVA or CM0.1, the density after foaming decreases with increasing pressure, temperature, and time. Among these factors, the effect of temperature is the most significant. The pore size is also closely related to the temperature, increasing with higher temperatures. Additionally, the cell density of EVA after foaming varies significantly under different conditions, while CM0.1 exhibits a relatively stable state. The density of the pure EVA foam material ranged from 0.223 to 0.669 g/cm^3, while that of CM0.1 ranged from 0.193 to 0.531 g/cm^3. This suggests that the density of CM0.1 foam material is lower than that of pure EVA, and the distribution range of CM0.1 is relatively narrow.

Moreover, the pore size of the pure EVA foam material ranged from 1.90 to 5.17 μm, while that of CM0.1 ranged from 1.74 to 3.57 μm. These results demonstrate that the pore size of CM0.1 foam material is smaller than that of pure EVA, and the size deviation of CM0.1 is also smaller. Additionally, the cell density of the pure EVA foam material ranged from 1.61×10^{10} to 2.10×10^{11} $cells/cm^3$, whereas for CM0.1, it ranged from 9.18×10^{10} to 3.23×10^{11} $cells/cm^3$.

Therefore, the cell density of CM0.1 foam material is higher than that of pure EVA. Introducing numerous tiny pores within the polymer achieves a reduction in density, resulting in a weight-reduction effect. When the foamed material is subjected to impact, the gas within the bubbles undergoes stagnation and compression, dissipating and consuming the incoming energy. Microcellular foams with high cell densities offer reduced material costs and superior mechanical performance. This makes them highly competitive in various applications, including sporting equipment, automotive, construction, and more [26].

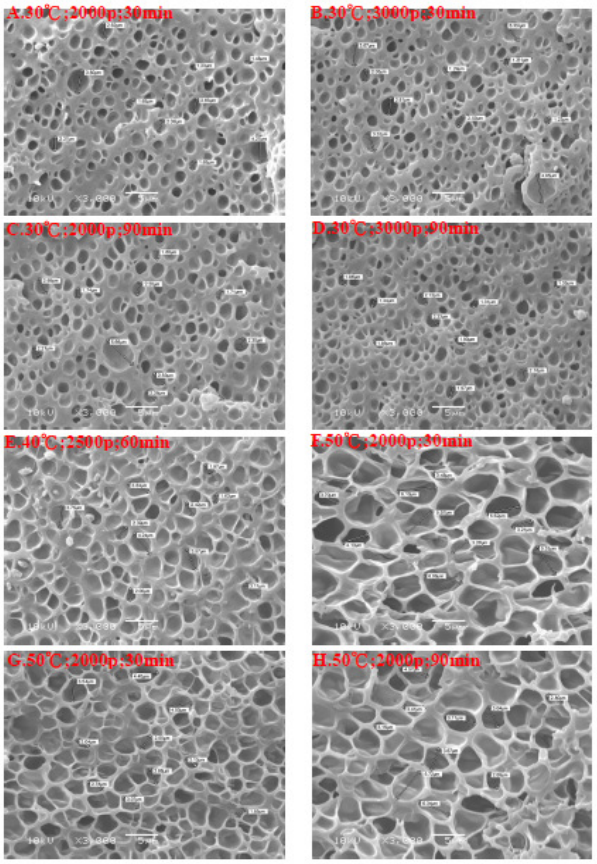

Fig. 10 SEM diagram of EVA foam material

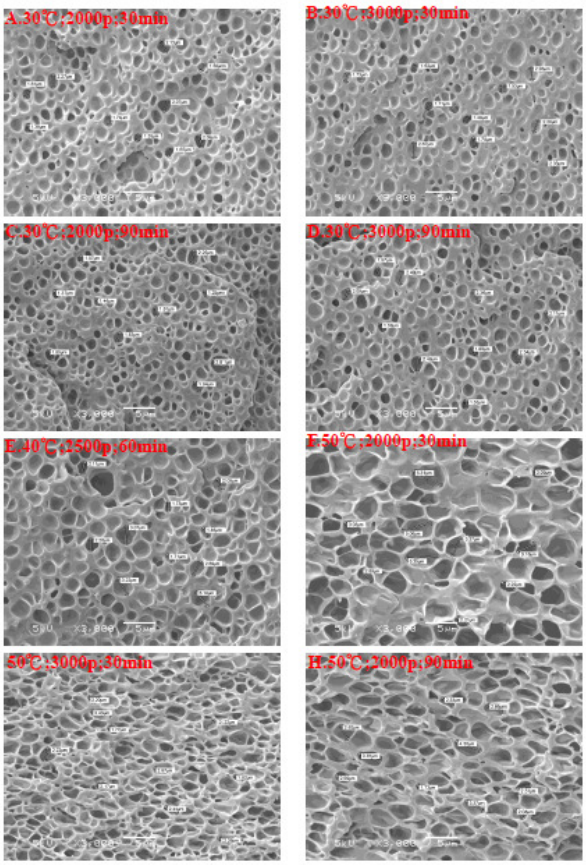

Fig. 11 SEM diagram of CM0.1 foam material

Fig. 10 depicts the SEM image of the foam material obtained from pure EVA under various temperatures, pressure, and time conditions. It is observed that at 30 °C, the cell size is significantly smaller compared to that at 50 °C. However, it can be noticed that the gap between the cells and the cell walls is considerably thicker at 30 °C than at 50 °C. This phenomenon suggests that at lower temperatures, the polymer exhibits a state of solid-liquid coexistence, where the melted polymer and carbon dioxide are unable to be effectively released during the foaming process. As a result, the gap thickness between the cells becomes enlarged.

Fig. 11 presents the SEM image of the foam material produced from CM0.1 under varying temperatures, pressure, and time conditions. It can be observed that the cell size in CM0.1 foam material is more uniform and denser compared to pure EVA. The cell density of the CM0.1 foam is larger than that of the EVA foam because the addition of nanocellulose improves the melt viscoelasticity, subsequently enhancing the melt strength. This improvement may be beneficial for suppressing cell coalescence [27]. Based on the aforementioned results, it can be inferred that the addition of modified carrot nanocellulose to EVA enhances the melt strength of the polymer, leading to improved foaming characteristics of the material.

Moreover, Li et al. [15] investigated the supercritical CO_2 foaming behavior and foam properties of EVA/ZnO composites, and their results showed that the pore size was 50.4 ± 11.7 μm by the addition of 5 wt% of ZnO, and the cell density was 5.3×10^7 cells/cm^3. Compared with these results, it can be observed that the addition of CM to EVA exhibited better foam characteristics, including a smaller pore size and higher cell density.

4. Conclusions

The average diameters of the unmodified and modified carrot nanocelluloses were 24.35 ± 3.15 nm and 30.45 ± 1.86 nm, respectively. The mechanical property analysis demonstrates a significant reinforcing effect with the addition of a small amount of nanocellulose (0.2 wt%) to EVA. Specifically, the tensile strength of EVA can be increased by 29.84 % when 0.2 wt% of MMA-modified nanocellulose is added. This confirms that the modification enhances the hydrophobicity of the nanocellulose, thereby improving its compatibility with EVA and increasing its mechanical strength. Furthermore, the incorporation of modified carrot nanocellulose into EVA improves the melt strength of the polymer during supercritical CO_2 foaming, resulting in a more consistent cell size and higher cell density. The results showed that adding nanocellulose can indeed enhance the properties of physically foamed materials.

Therefore, future studies will continue with further research on other formulations for physical foaming. These nanocomposites not only modify the mechanical properties of EVA but also effectively recycle carrot waste, promoting environmental protection.

Conflicts of Interest

The authors declare no conflict of interest.

References

[1] I. M. T. Usman, Y. C. Ho, L. Baloo, M. K. Lam, and W. Sujarwo, "A Comprehensive Review on the Advances of Bioproducts from Biomass towards Meeting Net Zero Carbon Emissions (NZCE)," Bioresource Technology, vol. 366, article no. 128167, December 2022.

[2] P. S. Sadalage and K. D. Pawar, "Production of Microcrystalline Cellulose and Bacterial Nanocellulose through Biological Valorization of Lignocellulosic Biomass Wastes," Journal of Cleaner Production, vol. 327, article no. 129462, December 2021.

[3] G. Siqueira, K. Oksman, S. K. Tadokoro, and A. P. Mathew, "Re-Dispersible Carrot Nanofibers with High Mechanical Properties and Reinforcing Capacity for Use in Composite Materials," Composites Science and Technology, vol. 123, pp. 49-56, February 2016.

[4] A. Horta-Velázquez and E. Morales-Narváez, "Nanocellulose in Wearable Sensors," Green Analytical Chemistry, vol. 1, article no. 100009, April 2022.

[5] S. Mondal, "Preparation, Properties and Applications of Nanocellulosic Materials," Carbohydrate Polymers, vol. 163, pp. 301-316, May 2017.

[6] T. Saito and A. Isogai, "Introduction of Aldehyde Groups on Surfaces of Native Cellulose Fibers by TEMPO-Mediated Oxidation," Colloids and Surfaces A: Physicochemical and Engineering Aspects, vol. 289, no. 1-3, pp. 219-225, October 2006.

[7] A. Isogai, T. Hänninen, S. Fujisawa, and T. Saito, "Catalytic Oxidation of Cellulose with Nitroxyl Radicals under Aqueous Conditions," Progress in Polymer Science, vol. 86, pp. 122-148, November 2018.

[8] S. Hu, Y. Zhi, S. Shan, and Y. Ni, "Research Progress of Smart Response Composite Hydrogels Based on Nanocellulose," Carbohydrate Polymers, vol. 275, article no. 118741, January 2022.

[9] M. K. Sinha, B. R. Das, D. Bharathi, N. E. Prasad, B. Kishore, P. Raj, et al., "Electrospun Nanofibrous Materials for Biomedical Textiles," Materials Today: Proceedings, vol. 21, part 4, pp. 1818-1826, 2020.

[10] Y. Jia and J. Zhang, "Thermal Conductivity of Ethylene-Vinyl Acetate Copolymers with Different Vinyl Acetate Contents Dependent on Temperature and Crystallinity," Thermochimica Acta, vol. 708, article no. 179141, February 2022.

[11] A. R. Carmona and H. A. C. Lopera, "A New Composite Made from Luffa Cylindrica and Ethylene Vinyl Acetate (EVA): Mechanical and Structural Characterization for Its Use as Mouthguard (MG)," Journal of the Mechanical Behavior of Biomedical Materials, vol. 126, article no. 105064, February 2022.

[12] K. Park, K. Sadeghi, P. K. Panda, J. Seo, and J. Seo, "Ethylene Vinyl Acetate/Low-Density Polyethylene/Oyster Shell Powder Composite Films: Preparation, Characterization, and Antimicrobial Properties for Biomedical Applications," Journal of the Taiwan Institute of Chemical Engineers, vol. 134, article no. 104301, May 2022.

[13] P. W. Anggoro, A. A. Anthony, M. Tauviqirrahman, Jamari, A. P. Bayuseno, and A. Han, "Machining Parameter Optimization of EVA Foam Orthotic Shoe Insoles," International Journal of Engineering and Technology Innovation, vol. 10, no. 3, pp. 179-190, July 2020.

[14] C. Z. P. Junior, R. S. Peruchi, F. de Carvalho Fim, W. D. O. S. Soares, and L. B. da Silva, "Performance of Ethylene Vinyl Acetate Waste (EVA-w) When Incorporated into Expanded EVA Foam for Footwear," Journal of Cleaner Production, vol. 317, article no. 128352, October 2021.

[15] N. Li, D. Fan, Z. Shi, Y. Xie, M. Li, and T. Tang, "Effect of Ion-Crosslinking on Supercritical CO2 Foaming Behavior and Foam Properties of EVA/ZnO Composites," Composites Communications, vol. 25, article no. 100760, June 2021.

[16] A. Briand, A. Leybros, O. Doucet, M. Vite, A. Gasmi, J. C. Ruiz, et al., "Deformation-Induced Delamination of Photovoltaic Modules by Foaming Ethylene-Vinyl Acetate with Supercritical CO2," Journal of CO2 Utilization, vol. 59, article no. 101933, May 2022.

[17] Q. Ren, M. Wu, L. Wang, W. Zheng, Y. Hikima, T. Semba, et al., "Cellulose Nanofiber Reinforced Poly (Lactic Acid) with Enhanced Rheology, Crystallization and Foaming Ability," Carbohydrate Polymers, vol. 286, article no. 119320, June 2022.

[18] Y. F. Shih, Z. Z. Lai, and V. K. Kotharangannagari, "Preparation and Characterization of Carrot Nanofiber and Their Reinforced Nanocomposite Films," Key Engineering Materials, vol. 845, pp 15-20, May 2020.

[19] Y. F. Shih, M. Y. Chou, H. Y. Lian, L. R. Hsu, and S. M. Chen-Wei, "Highly Transparent and Impact-Resistant PMMA Nanocomposites Reinforced by Cellulose Nanofibers of Pineapple Leaves Modified by Eco-Friendly Methods," eXPRESS Polymer Letters, vol. 12, no. 9, pp. 844-854, September 2018.

[20] Y. F. Shih, V. K. Kotharangannagari, and T. C. Tsou, "Development of Eco-Friendly Modified Cellulose Nanofiber Reinforced Polystyrene Nanocomposites: Thermal, Mechanical, and Optical Properties," Journal of Polymer Research, vol. 27, no. 7, article no.181, July 2020.

[21] H. N. Day, S. J. Hsiao, C. C. Tsao, W. C. Liang, S. J. Liou, and C. L. Wu, Manufacturing Method for Foaming Shoe Materials, T.W. Patent, TWI519401B, February 01, 2016.

[22] K. H. Ho, M. van Meurs, X. Lu, and S. K. Lau, "Interfacial Stabilizing and Reinforcing Effects of Silsesquioxane-Based Hybrid Janus Molecules in Extrusion Supercritical CO2 Foaming of Polypropylene," Materials & Design, vol. 224, article no. 111345, December 2022.

[23] M. A. Adekoya, S. Liu, S. S. Oluyamo, O. T. Oyeleye, and R. T. Ogundare, "Influence of Size Classifications on the Crystallinity Index of Albizia gummifera Cellulose," Heliyon, vol. 8, no. 12, article no. e12019, December 2022.

[24] D. Lin, Y. Li, Y. Huang, W. Qin, D. A. Loy, H. Chen, et al., "Properties of Polyvinyl Alcohol Films Reinforced by Citric Acid Modified Cellulose Nanocrystals and Silica Aerogels," Carbohydrate Polymers, vol. 298, article no. 120116, December 2022.

[25] Y. F. Shih, M. Y. Chou, W. C. Chang, H. Y. Lian, and C. M. Chen, "Completely Biodegradable Composites Reinforced by the Cellulose Nanofibers of Pineapple Leaves Modified by Eco-Friendly Methods," Journal of Polymer Research, vol. 24, no. 11, article no. 209, November 2017.

[26] W. Zhai, J. Yu, and J. He, "Ultrasonic Irradiation Enhanced Cell Nucleation: An Effective Approach to Microcellular Foams of Both High Cell Density and Expansion Ratio," Polymer, vol. 49, no. 10, pp. 2430-2434, May 2008.

[27] P. Huang, Y. Su, F. Wu, P. C. Lee, H. Luo, X. Lan, et al., "Extruded Polypropylene Foams with Radially Gradient Porous Structures and Selective Filtration Property via Supercritical CO2 Foaming," Journal of CO2 Utilization, vol. 60, article no. 101995, June 2022.